World Academy of Science, Engineering and Technology
International Journal of Mechanical and Mechatronics Engineering
Vol:7, No:1, 2013

Microstructure and Mechanical Characterization of Heat Treated Stir Cast Silica (Sea Sand) Reinforced 7XXX Al Alloy MMCs

S. S. Sharma, Jagannath K, P. R. Prabhu

Open Science Index, Mechanical and Mechatronics Engineering Vol:7, No:1, 2013 publications.waset.org/9996749.pdf

***Abstract*—**Metal matrix composites consists of a metallic matrix combined with dispersed particulate phase as reinforcement. Aluminum alloys have been the primary material of choice for structural components of aircraft since about 1930. Well known performance characteristics, known fabrication costs, design experience, and established manufacturing methods and facilities, are just a few of the reasons for the continued confidence in 7XXX Al alloys that will ensure their use in significant quantities for the time to come. Particulate MMCs are of special interest owing to the low cost of their raw materials (primarily natural river sand here) and their ease of fabrication, making them suitable for applications requiring relatively high volume production. 7XXX Al alloys are precipitation hardenable and therefore amenable for thermomechanical treatment. Al–Zn alloys reinforced with particulate materials are used in aerospace industries in spite of the drawbacks of susceptibility to stress corrosion, poor wettability, poor weldability and poor fatigue resistance. The resistance offered by these particulates for the moving dislocations impart secondary hardening in turn contributes strain hardening. Cold deformation increases lattice defects, which in turn improves the properties of solution treated alloy. In view of this, six different Al–Zn–Mg alloy composites reinforced with silica (3 wt. % and 5 wt. %) are prepared by conventional semisolid synthesizing process. The cast alloys are solution treated and aged. The solution treated alloys are further severely cold rolled to enhance the properties. The hardness and strength values are analyzed and compared with silica free Al – Zn-Mg alloys. Precipitation hardening phenomena is accelerated due to the increased number of potential sites for precipitation. Higher peak hardness and lesser aging time are the characteristics of thermo mechanically treated samples. For obtaining maximum hardness, optimum number and volume of precipitate particles are required. The Al-5Zn-1Mg with 5% SiO_2 alloy composite shows better result.

***Keywords*—**Dislocation, hardness, matrix, thermomechanical, precipitation hardening, reinforcement.

I. INTRODUCTION

THE properties of various aluminum alloys can be altered by age hardening heat treatment. The age hardening heat treatment can be classified into two processes, including solution heat treatment and artificial aging [1]-[5]. This consists of heating the alloy to a temperature between 300 to 450°C at which all the alloying elements are in solution. By heating the solution treated material to a temperature above room temperature and holding it there, the precipitation of intermetallics accelerates and the strength is further increased compared to natural aging and accompanied by a clear drop in ductility [6]-[9]. This is called ‘‘artificial aging’’, ‘‘age hardening’’ or just ‘‘aging’’ and is generally carried out at temperatures up to approximately 200°C. Age hardening Al–Zn–Mg series alloys have been widely used as structural materials in the aerospace and automotive industries due to the attractive combined properties, such as low density, high strength, hardness, ductility and toughness. In recent years, aluminum alloys have attracted attention of many researchers, engineers and designers as promising structural materials for automotive industry or aerospace applications [10-12].

Thermomechanical treatment (TMT) consists of deforming the metal between the solution treatment and the aging treatment in thermomechanical processing of precipitation hardenable alloys. Low temperature thermomechanical treatment (LTMT) is concerned about cold deformation of the metal. The effect of deformation on precipitation kinetics has often been attributed to an increase of dislocation density, which increases the nucleation sites, for phase transformation and provides easy diffusion paths for precipitation-forming elements in the material, leading to accelerated precipitation process as compared with the undeformed alloy. It is also believed that the precipitation process can still be promoted even when the dislocations formed during deformation have been eliminated before the precipitation starts [13]. Therefore, the effect of deformation on the precipitation cannot be explained from dislocation density considerations alone. Some experimental observations have suggested that deformation can cause the redistribution of the precipitate forming elements between the dislocation cell walls and the cell interiors. Thus segregation of the solute atoms to the potential nucleation sites may also contribute to precipitation kinetics and could provide an explanation for the observed acceleration of the precipitation process [14], [15]. It is clear that cold working enhances precipitation of strengthening phases, which has been put to good use for many years for achieving superior properties in various Al alloys and composites. This relationship between cold working and precipitation is used advantageously in tailoring the properties of these materials in order to overcome the specific problems.

S. S. Sharma and Jagannath K are Professors with the Department of Mechanical& Manufacturing Engineering, Manipal Institute of Technology, Manipal - 576104 (Phone: 0820 2925473; Fax: 0820 292571071; e-mail: ss.sharma@manipal.edu, jagan.korody@manipal.edu).

P. R. Prabhu, Asst. Professor – seniorscale, Department of Mechanical & Manufacturing Engineering, Manipal Institute of Technology, Manipal - 576104 (e-mail: raghuprabhu123@gmail.com).

II. EXPERIMENTAL DETAILS

A. Alloy Preparation

Six types of Al alloy composites are cast in the laboratory by Stir casting technique and are solidified in the crucible itself. Table I shows the composition of the alloys/composites. The cast metal is cut into small test pieces of 25mm x 20mm x 10mm.

TABLE I
COMPOSITION OF 6 TYPES OF ALLOYS/COMPOSITES USED IN THIS STUDY

Type	Chemical composition
A	Al – 10Zn-1Mg
B	Al–10Zn –1Mg - 3 SiO_2
C	Al–10Zn –1Mg - 5 SiO_2
D	Al–5Zn –1Mg
E	Al–5Zn –1Mg - SiO_2
F	Al–5Zn –1Mg - SiO_2

B. Homogenizing Treatment

Specimens are heated isothermally for 12 hours at 400°C. To minimize the oxidation of the alloy, the fusible salt bath of $NaNO_2$ and KNO_3 is used. At such a high temperature the solute clusters are eliminated and homogeneous chemical composition is obtained.

C. Deformation to Suitable Initial Size

During deformation to reduce the specimen thickness from 10mm to 2mm, severe strain hardening is observed and specimen used to fail during cold rolling. Intermediate annealing treatment of 2 hours at 350°C was carried out to nullify the work hardening effect. Initial specimen thickness for 33% and 50% deformation is 3mm and 4mm respectively.

D. Conventional Precipitation Hardening Treatment

Specimens are first heated to 350°C in salt bath and quenched in cold water. This solution treated samples are aged at 50°C and 100°C and hardness versus aging duration graphs are plotted for all six types of specimens.

E. Thermomechanical Treatment

All the specimens are cold rolled after solution treatment with 33 and 50% of deformation to reduce the thickness to 2mm. At the end, rolling is performed through several passes giving only a small amount of reduction in each pass without any intermediate annealing treatment. These strained samples are aged at 50°C and 100°C and hardness versus aging duration graphs are plotted.

F. Hardness Measurement

All the treated and untreated specimens are subjected to Rockwell hardness test and the “B” scale hardness numbers are noted.

G. Tensile Test

First, tensile specimens are prepared. Size and shape of the specimens is shown in Fig. 1. Tension test is carried out on laboratory UTM of 100KN capacity (made by INSTRON) at cross head speed of 5mm/minute. Yield strength is taken as 2% proof stress. Yield strength, UTS, and % elongation are found for some selected specimens.

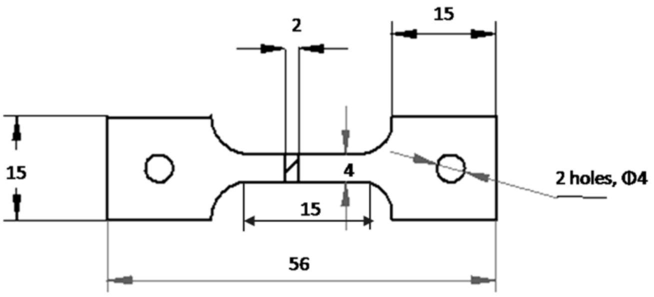

Fig. 1 Tensile testspecimen (all dimensions in mm)

H. Wear Test

The dry sliding wear behavior is analyzed here. Before taking the reading, a trail run of 30mins is provided to all the specimens to develop a perfectly flat and smooth contact surface. The experiment is conducted on pin-on-disc apparatus for 1hr 15mins each on all specimens and the weight loss is noted at every 15mins run of the specimen. Shape and size of the specimen used for wear test is shown in Fig. 2. Specimen is joined to steel shank by the adhesive. Calculation of the sliding distance in KM is shown below.

$$\text{Sliding speed in m/sec} = \frac{\pi DN}{60,000} \tag{1}$$

where, D = diameter of wear track in mm (88mm), T = test duration in seconds (15mins), N = RPM of disc (200), Sliding distance for 15mins is 3.317KM

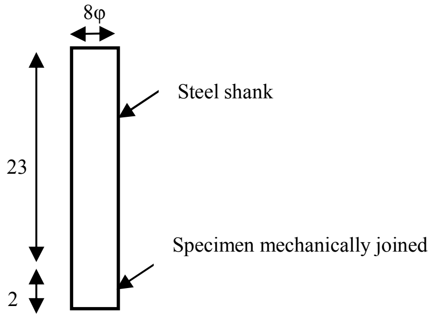

Fig. 2 Wear testing specimen (all dimensions in mm)

1. Microstructure Analysis

Specimens are polished and etched with Keller’s reagent [2ml HF (48%conc.), 3ml HCl (conc.), 5ml HNO3 (conc.) and 190ml water]. Microstructures of homogenized specimens are recorded in metallurgical microscope at 300X magnification.

III. RESULTS AND DISCUSSIONS

A. Hardness Measurement

Fig. 3 shows the hardness curves with the aging duration for “A” type alloy. Similarly graphs are drawn for all the other alloys/composites and peak hardness values are noted. Peak hardness value increases with the increase in degree of deformation and decrease in aging temperature. In conventional aging, lower aging temperature increases the peak hardness value but with the longer aging duration. Increase in peak hardness value is due to the increase in the number of intermediate transition zones during the formation of intermetallic phases. Figs. 4 to 9 show the peak hardness values of respective alloys/composites with the modification in heat treatment. Compared to Al-10%Zn alloy group, Al-5%Zn alloy group shows increased hardness. Also silica reinforcement increases the response of alloy to TMT. The alloy Al-5Zn-1Mg-5 SiO_2 shows the highest peak hardness values in the Al-Zn-Mg group composites. An optimum number of optimum sized well distributed intermetallics in the matrix contribute a lot to the increased strength and hardness. Literature also indicated the presence of $MgZn_2$, $Mg_3Zn_3Al_2$ intermetallics in such alloy systems.

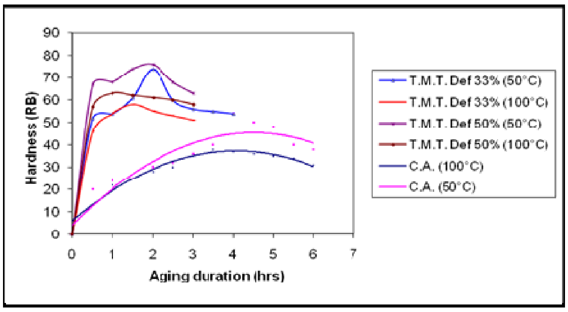

Fig. 3 Variation of hardness with the aging duration

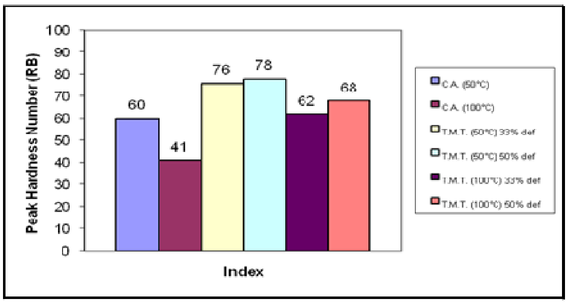

Fig. 4 Variation of peak hardness of "A" type composite with the modification in heat treatment

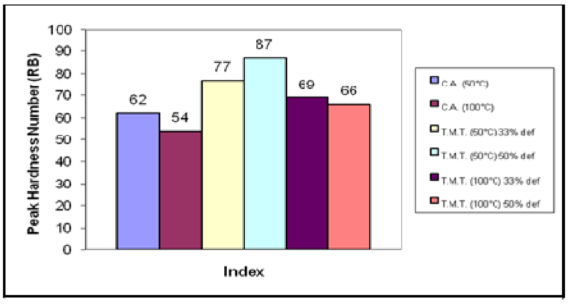

Fig. 5 Variation of peak hardness of "B" type composite with the modification in heat treatment

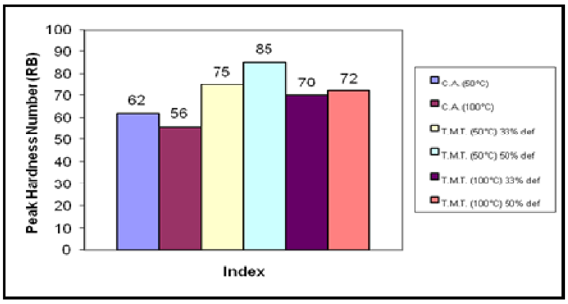

Fig. 6 Variation of peak hardness of "C" type composite with the modification in heat treatment

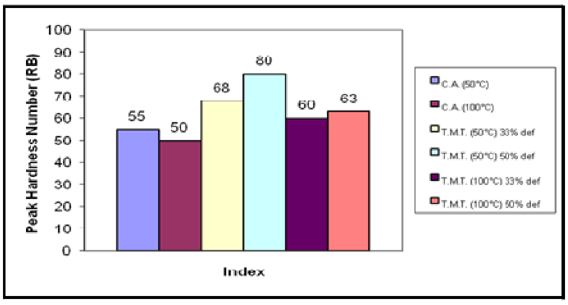

Fig. 7 Variation of peak hardness of "D" type composite with the modification in heat treatment

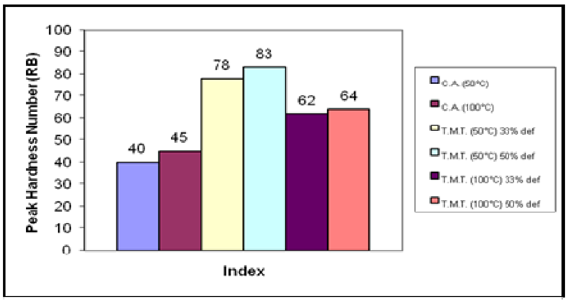

Fig. 8 Variation of peak hardness of "E" type composite with the modification in heat treatment

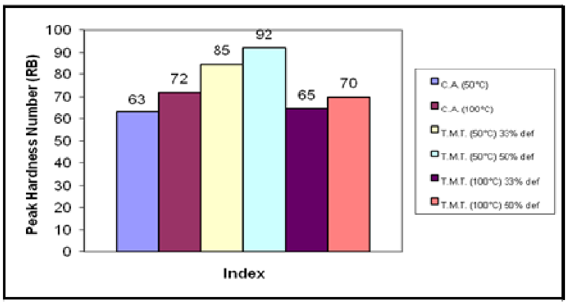

Fig. 9 Variation of peak hardness of "F" type composite with the modification in heat treatment

B. Tensile Test

Fig. 10 shows the yield strength variation of thermomechanically treated alloys. Fig. 11 shows the UTS variation of thermomechanically treated samples. All the tensile graphs show the increase in tensile values with the increase in degree of cold deformation. Al-5Zn-1Mg-5SiO_2

showed best results. This also supports the argument that fine, well distributed optimum numbers of particles are responsible to the increase in strength. Fig. 12 shows the variation in ductility values with the thermomechanically treated specimens. Surprisingly the addition of $5SiO_2$ to Al-5Zn-1Mg composite shows an increase in ductility value over other composites in spite of an increase in strength and hardness values. So if the TMT is properly tailored in the Al alloy with an optimum number of Zn &SiO_2 content, the ductility, hardness strength can be improved.

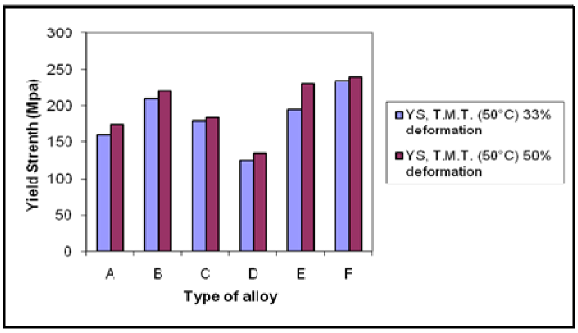

Fig. 10 Yield strength variation of thermomechanically treated composites

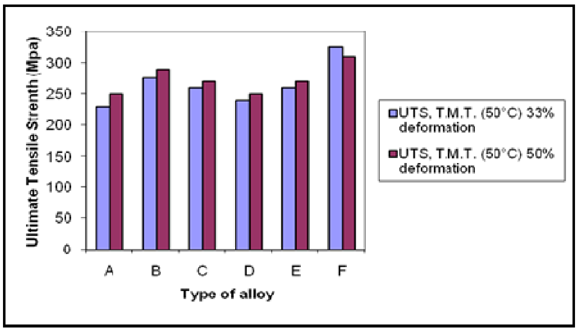

Fig. 11 UTS variation of thermomechanically treated composites

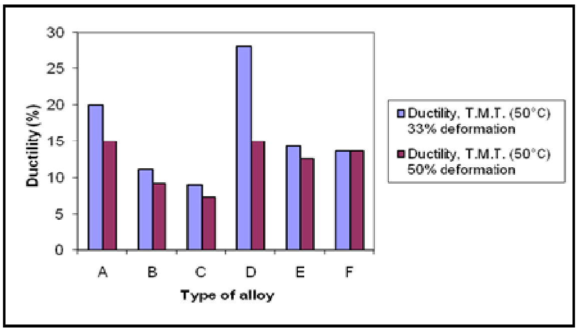

Fig. 12 Variation in ductility with the thermomechanically treated composites

C. Wear Test

Figs. 13 to 18 show the cumulative wear versus sliding distance graphs for all the six types of specimens with different heat treatment conditions. Wear is generally the function of hardness. In all the cases, conventionally aged at 100°C specimens show least resistance to wear. Thermomechanically treated specimen with high degree of deformation and aged at lower temperature showed higher wear resistance. All the specimens contribute higher wear resistance when thermomechanically treated with high degree of deformation, Al-5Zn-1Mg-$5SiO_2$ specimen emerged as highest wear resistance material in the group. As the hardness increases, the wear resistance of the specimen also increases. Increase in wear resistance and the mechanical properties are due to the combined effect of dislocations with the precipitating secondary phases (intermetallics).

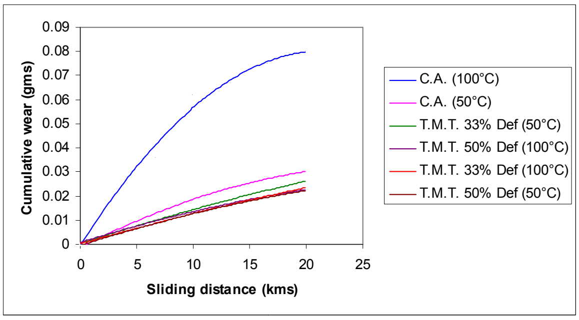

Fig. 13 Cumulative wear versus sliding distance of “A” type composite

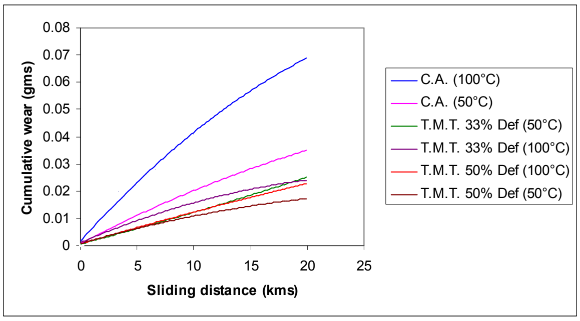

Fig. 14 Cumulative wear versus sliding distance of “B” type composite

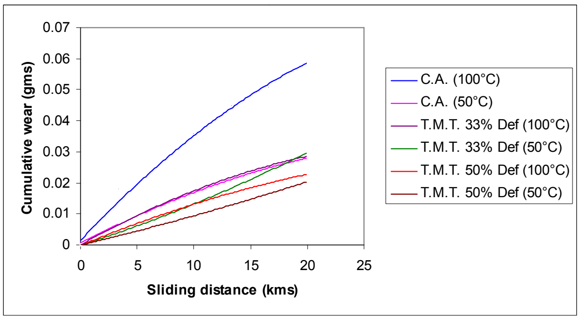

Fig. 15 Cumulative wear versus sliding distance of “C” type composite

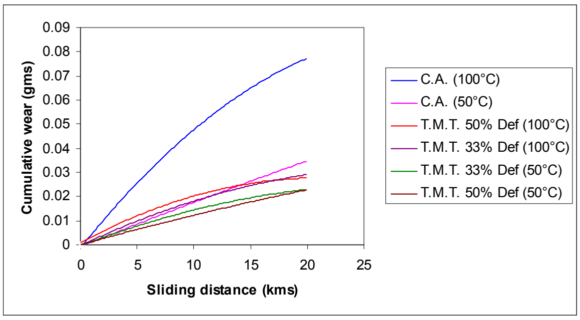

Fig. 16 Cumulative wear versus sliding distance of “D” type composite

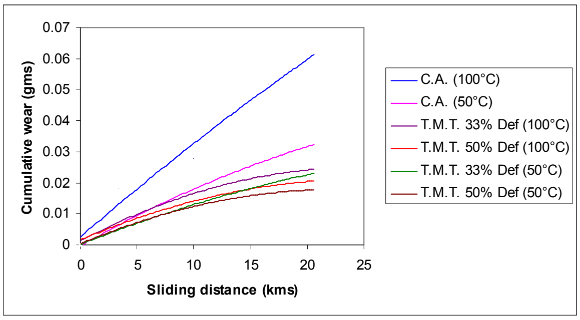

Fig. 17 Cumulative wear versus sliding distance of “E” type composite

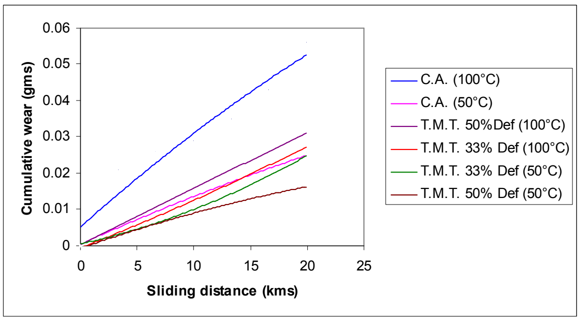

Fig. 18 Cumulative wear versus sliding distance of “F” type composite

D. Microstructure Analysis

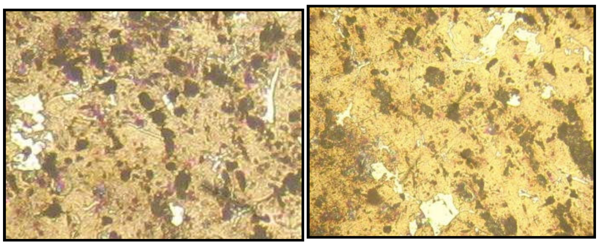

Fig. 19 (a) Microstructure of homogenized “F” type composite (b) Microstructure of homogenized “C” type composite

Fig. 19 shows the microstructure of F and C type composites at 300X magnification after homogenizing. Homogenized microstructure shows equiaxial grains without any dendritic segregation.

IV. CONCLUSIONS

- Lower aging temperature increases the peak hardness values with increased peak aging duration.
- Thermomechanically treated specimens show higher peak hardness values with decreased peak aging duration.
- In TMT, as the degree of cold deformation increases or aging temperature decreases, the peak hardness values increase.
- Yield strength and ultimate tensile strength are higher for thermomechanically treated specimen with higher degree of deformation.
- TMT improves strength and hardness to higher values compared to conventional aging.
- As the weight percentage of magnesium increases in the alloy, the hardness, strength, wear resistance increase with the decrease in ductility.
- With the same magnesium weight percentage in the alloy, an optimum weight percentage of Zinc (5%) is required to get better combination of properties.
- Al-5Zn-1Mg-5SiO$_2$ alloy shows the best combination of properties like strength, hardness, wear resistance and ductility.
- Thermomechanical treatment improves ductility with higher hardness and strength if it is properly designed.
- Homogenizing treatment is required to eliminate dendritic segregation.

REFERENCES

[1] De Sanctis M, *“Structure and properties of rapidly solidified ultrahigh strength Al–Zn–Mg–Cu alloys produced by spray deposition”, Material Science Engineering* 1991; A141:103–21.

[2] Duan X, Hao Y, Yoshida M, Ando T, Grant N. J, *“Liquid dynamic compaction of aluminum alloy 7150”, International Journal of Powder Metallurgy* 1993;29(2): 149–59.

[3] Lengsfeld P, Juarez-Lslas J. A, Cassada W. A, Lavernia E.J. *“Microstructure and mechanical behavior of spray deposited Zn modified 7XXX series Al alloys”, International Journal of Rapid Solidification* 1995; 8: 237–65.

[4] Li X. Z, Hansen V, Gjonnes J, Wallenberg L. R, *“HREM study and structure modeling of the g0 phase, the hardening precipitates in commercial Al–Zn–Mg alloys”,* Acta Mater 1999;47(9):2651–9.

[5] Troeger L. P, Starke E. A., *“Microstructural and mechanical characterization of a superplastic 6xxx aluminum alloy”, Material Science Engineering A* 2000; 277: 102–13.

[6] Berg L. K, Gjonnes J, Hansen V, Li X. Z, Knutson-wedel M, Waterloo G, et al. *“GP-zones in Al–Zn–Mg alloys and their role in artificial aging” Acta Mater* 2001;49:3443–34651

[7] Song R. G, Zhang Q. Z, *“Heat treatment optimization for 7175 aluminum alloy by genetic algorithm. Material Science Engineering, C* 2001; 17:133–7.

[8] TangenStian, Sjolstad Knut, Nes Erik, FuruTrond, Marthinsen Knut, *“The effect of precipitation on the recrystallization behavior of a supersaturated, cold rolled AA3103 aluminium alloy”, Material Science Forum* 2002;396–402:469.

[9] Lee S. H, Saito Y, Sakai T, Utsunomiya H, *“Microstructures and mechanical properties of 6061 aluminum alloy processed by accumulative roll-bonding”, Material Science Engineering A* 2002;325:228–35.

[10] Robson J. D, *“Optimizing the homogenization of zirconium containing commercial aluminium alloys using a novel process model”, Material Science Engineering A* 2002; 338:219–29.

[11] Chen S. P, Kuijpers NCW, van der Zwaag S, *“Effect of microsegregation and dislocations on the nucleation kinetics of*

precipitation in aluminium alloy AA3003", Material Science Engineering A 2003;341:296.

[12] Starink M. J, Wang S. C, *"A model for the yield strength of overaged Al–Zn–Mg–Cu alloys", Acta Mater* 2003;51:5131–50.

[13] Chen K. H, Liu H. W, Zhang Z, Li S, Todd R. I, *"The improvement of constituent dissolution and mechanical properties of 7055 aluminum alloy by stepped heat treatments", Journal of Material Process Technology,* 2003; 142:190–6.

[14] Dumont D, Deschamps A, Brechet Y, *"On the relationship between microstructure, strength and toughness in AA7050 aluminum alloy", Material Science Engineering A* 2003; 356: 326–36.

[15] Wang D, Nia D. R, Ma Z. Y, *"Effect of pre-strain and two-step aging on microstructure and stress corrosion cracking of 7050 alloy", Material Science Engineering A,* 2008.

Open Science Index, Mechanical and Mechatronics Engineering Vol:7, No:1, 2013 publications.waset.org/9996749.pdf